UDC 544.47 doi: 10.15407/hftp15.03.340

S.V. Prudius, N.L. Hes, A.Yu. Zhuravlov, V.V. Brei

OXIDATION OF XYLOSE – METHANOL MIXTURE INTO METHYL LACTATE AND METHYL GLYCOLATE ON CeO_2-SnO_2/AL_2O_3 CATALYST

Institute for Sorption and Problems of Endoecology of National Academy of Sciences of Ukraine
13 General Naumov Str., Kyiv, 03164, Ukraine, E-mail: svitprud@gmail.com

The development of catalytic methods for xylose transformation as renewable raw material into value-added chemicals such as lactic and glycolic acid esters has been the subject of intensive research in recent years. Thus, methyl lactate and methyl glycolate are used as a starting material for the production of lactide and glycolide – an important monomers for the production of biodegradable polymers. The aim of this work was to search of simple effective catalyst for transformation of xylose into methyl esters of lactic and glycolic acids. For this purpose, tin-containing alumina doped with CeO_2, MoO_3 and CuO oxides were synthesized by impregnation method. Textural and structural parameters of obtained MeO-SnO_2/Al_2O_3 mixed oxides were estimated from the results of low-temperature adsorption-desorption of nitrogen and X-ray diffraction. The formation of morphology ceria close to octahedra for CeO_2-SnO_2/Al_2O_3 sample is confirmed by the X-ray phase analysis data and SEM microphotographs. The UV spectroscopy data indicates the nanosize of tin dioxide particles on the γ-Al_2O_3 surface. According to the titration results, CeO_2-SnO_2/Al_2O_3 is acid mixed oxide with $H_0 \leq -3.0$. The catalytic conversion of xylose solution in methanol was carried out in rotated autoclaves and in a flow stainless steel reactor with a fixed bed of catalyst. The products of the target reaction $C_5H_{10}O_5+2CH_3OH+1/2O_2 = C_4H_8O_3+C_3H_6O_3+2H_2O$ were analyzed by ^{13}C NMR. It was found that a complete conversion of 4 % xylose solution in a 70 % aqueous methanol solution occurs with the formation of methyl lactate (42 %) and methyl glycolate (24 %) on the developed CeO_2-SnO_2/Al_2O_3 catalyst loading of 3.5 mmol $C_5H_{10}O_5/g_{cat}/h$ at 190 °C/3.0 MPa in air flow. The path of the reaction is proposed, namely: the $^{IV}Sn^{4+}$ ions in CeO_2-SnO_2/Al_2O_3 catalyst as Lewis acid sites promote retro-aldol xylose condensation and further Cannizzaro rearrangement of intermediate methyl pyruval hemiacetal into methyl lactate. And CeO_2 provides selective oxidation of glycol aldehyde formed as a result of aldol decondensation of xylose to methyl glycolate.

***Keywords**: xylose conversion, methyl lactate, methyl glycolate, mixed oxide, CeO_2, SnO_2*

INTRODUCTION

Xylose can be considered as a platform chemical, which is an intermediate to a plethora of chemicals such as xylitol, lactic acid and its esters and also furfural, in turn a key building block to produce several chemicals [1]. Lactic acid methyl ester, methyl lactate (ML), is used mainly as a cellulose acetate solvent [2] and as a starting material for the production of lactic acid oligomers and lactide [3, 4]. Methyl glycolate (MG), glycolic acid methyl ester, can be used as a good solvent instead of chlorinated hydrocarbons and as precursor for obtaining glycolide – an important monomer for the production of biodegradable polyglycolide [5].

The chemical ML or MG is usually produced by the esterification of lactic or glycolic acids with methanol [6]. Retro-aldol condensation of available hexose - glucose or fructose in the presence of methanol is a promising alternative way to obtaining methyl lactate, which has been developed recent years. In particular, we have found that SnO_2–containing oxides prepared by a simple wet impregnation of alumina provides 70 % yield of methyl lactate at 180 °C during continuous conversion of fructose in aqueous methanol solution [7]. In this article a possible scheme of fructose transformation into ethyl lactate on L-acid $^{IV}Sn^{4+}$ sites is presented. It was interesting to study similar transformation of pentose – xylose into esters of lactic and glycolic acids. In the case of xylose, retro-aldol splitting leads to C3 (glyceraldehyde) and C2 (glycol aldehyde) fragments. Further glyceraldehyde can dehydrate to methyl pyruvate that in the presence of methanol can rearrangement according to Cannizzaro into methyl lactate. But intermediate glycol aldehyde must be oxidized in the presence of methanol to methyl glycolate on appropriate catalysts. Thus, a studied reaction can be written as follows: $C_5H_{10}O_5+2CH_3OH+1/2O_2= C_4H_8O_3+C_3H_6O_3+2H_2O$. For glycol aldehyde

oxidation we have doped the SnO_2/Al_2O_3 catalyst with CeO_2, MoO_3 and CuO oxides as it is recommended in [8].

In this communication the results on transformation xylose-methanol mixture into methyl esters of lactic and glycolic acids over several mixed oxides supported by alumina are presented.

EXPERIMENTAL

MeO-SnO_2/Al_2O_3 mixed oxides were obtained by impregnating of granulated γ-Al_2O_3 (AOA, Ukraine) with an aqueous solution of salts $SnCl_4 \cdot 5H_2O$, $Ce(NO_3)_3 \cdot 6H_2O$, $Cu(NO_3)_2 \cdot 6H_2O$, $(NH)_6Mo_7O_{24} \cdot 4H_2O$ with subsequent heat treatment at 550 °C for 2 h. For impregnation, a fraction of 0.5–2.0 mm of carrier granules pre-dried at 250 °C was used. After calcination, the content of tin dioxide in the samples was 10 % by mass, and the content of other metal oxides was 5 %.

Thermal studies were carried out on a serial derivative Q-1500D (Hungary) in the temperature range of 290-1270 K using a platinum crucible. The sample heating rate was 10 K min^{-1}. The textural parameters of the oxides were determined by the method of low-temperature nitrogen adsorption-desorption on a Quantachrome Nova 2200e Surface Area and Pore Size Analyzer. To analyze the morphology of the sample, a high-resolution auto-emission scanning electron microscope (SEM JSM-6700, JEOL, Japan) with energy-dispersive and cathode-luminescent attachments was used (resolution 1.0–2.2 nm). X-ray patterns of the catalysts were recorded on a DRON-4-07 diffractometer in the Cu K_α line of the anode with a nickel filter in the reflected beam with the Bragg-Brentano shooting geometry. Diffuse reflectance UV-Vis spectra were recorded using a Perkin Elmer Lambda 40 spectrophotometer equipped with a diffuse reflectance camera and an integrating sphere (Labsphere RSA-PE-20). MgO was used as a standard. To determine the band gap E_0, the reflection spectra were converted to the absorption spectra using the Kubelka–Munk formula, $F = (h\nu(1 - R)^2/2R)^{1/2}$. The value of E_0 was determined from the almost linear long-wavelength segment of the absorption band section, extrapolated to the intercept with the abscissa. The strength of the acid sites of the samples in terms of the Hammett H_0 function was determined according to the standard method using the appropriate Hammett indicators (Aldrich) [9]. To determine the total concentration of acid sites, the method of reverse titration of *n*-butylamine adsorbed on the surface of the samples with a solution of hydrochloric acid in the presence of the indicator bromothymol blue [9] was used.

The catalytic conversion of a 10 % xylose solution (*h*) in a methanol was previously carried out in autoclaves with Teflon liners (25 ml) with rotation at a speed of 60 rpm for a certain time at the temperature of 160 °C, 3 h. Further, the catalytic experiment was carried out in a stainless-steel flow reactor with a diameter of 8 mm with a fixed catalyst layer (1.7 g, 3 cm^3) at temperatures of 160–190 °C and the pressure of 3.0 MPa. The reaction mixture (4 % xylose solution in a 70 % aqueous methanol solution) for contact with the heated catalyst layer was fed from top to bottom using a Waters-590 pump with the same volume velocity LHSV = 4÷6 h^{-1}, which corresponded to a feed rate of 2÷3.5 mmol $C_5H_{10}O_5/g_{cat}$/h interval. Air was used as a carrier gas, with air oxygen serving as an oxidizer. Under these conditions, the components of the initial solution and transformation products were in a liquid state.

The xylose conversion products were identified by ^{13}C NMR spectra ("Bruker Avance-400" spectrometer Karlsruhe, Germany) and by liquid chromatography (Waters HPLC system; Alliance, MA, USA). Xylose conversion (%) and product selectivity (mol %) were calculated from ^{13}C NMR spectra by the corresponding ratio of the planes of the signals of methyl lactate at 67 ppm, methyl glycolate at 60 ppm, and methyl formate at 51 ppm. Calibration ^{13}C NMR spectra of mixtures of methyl lactate : methyl glycolate : xylose with given molar ratios of components of 0.5:1:1were previously recorded. Xylose conversion (X) and product selectivity (*Y*, mol %) were calculated according to Eqs:

$$X\ (\text{mol}\%) = \frac{[xylose]i - [xylose]pr}{[xylose]i} * 100,$$

$$S\ (\text{mol}\%) = *100.$$

RESULTS

The results of thermal analysis of the not-calcined samples are shown in Fig. 1. In the derivatograms of the CeO_2-SnO_2/Al_2O_3 and CuO-SnO_2/Al_2O_3 samples, only one endothermic effect was observed with mass loss in the region of 140–180 °C, caused by the condensation of

structural OH-groups with water release. The total weight loss of samples after heating to 1000 °C is 16.6 and 31.9 % by mass respectively. For the MoO_3-SnO_2/Al_2O_3 sample, two additional endo-effects appear with mass loss at 300 and ~ 375 °C, caused by the decomposition of the deposited molybdenum (VI) salt [10]. The total weight loss of the sample after heating to 1000 °C is 39.7 % by mass. Thermogravimetric data showed the same good trend in thermal stability of all prepared samples.

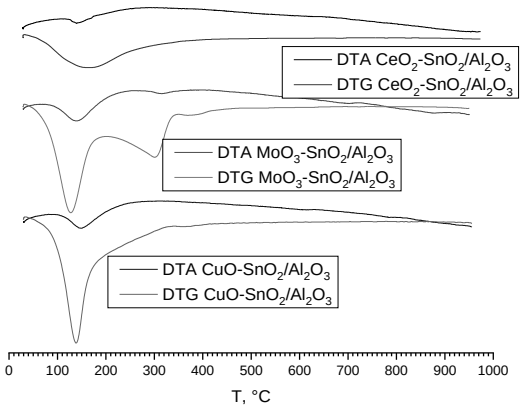

Fig. 1. The TGA/DTG curves of MeO-SnO_2/Al_2O_3 samples, dried at 120 °C (4 h) (heating rate - 10 °C/min)

As can be seen from the diffraction patterns (Fig. 2) of SnO_2/Al_2O_3 and MoO_3-SnO_2/Al_2O_3 samples, no crystalline Sn or Mo species could be detected, that indicates their well dispersed on the alumina surface forming small domains not detectable by XRD. It is interesting that the CuO-SnO_2/Al_2O_3 spectrum reveals the formation of the tetragonal rutile SnO_2 (JCPDS–41-1445) crystal structure and space group–P42/mnm, indicates by narrow peaks centered about 26.6°; 33.9°; 38.0° and 51.8 [11]. The introduction of copper oxide promotes the agglomeration of SnO_2 particles in the CuO-SnO_2/Al_2O_3 sample, while no peaks characteristic of CuO are observed. For the CeO_2-SnO_2/Al_2O_3 sample intense diffraction peaks at 28.66°; 33.08°; 47.47°; 56.36°; 59.08°; 69.40°; 76.70°; 79.07° and 88.41° are observed, which correspond to the cubic fluorite phase CeO_2 (JCPDS–34-0394) and space group–Fm3m [12]. Wherein there are no any characteristic peaks belong to SnO_2. The main intensive diffraction peak located at $2\theta = 28.66°$ corresponds to the (111) facet, that is the most thermodynamically stable [13]. It is known that the (111) facet is exposed when CeO_2 crystals have the shape of octahedra.

The formation of morphology ceria close to octahedra is confirmed by SEM microphotographs of the CeO_2-SnO_2/Al_2O_3 sample (Fig. 3).

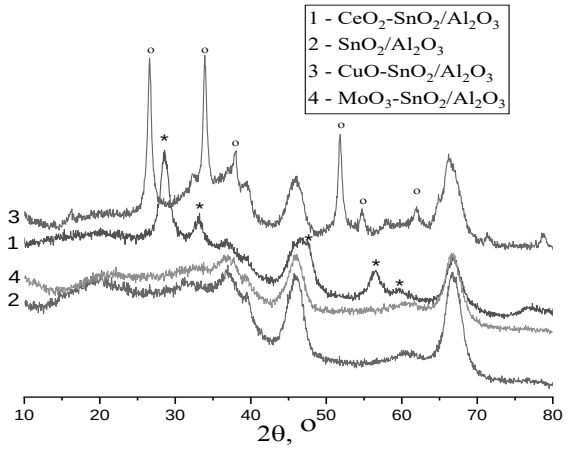

Fig. 2. XRD spectra of MeO-SnO_2/Al_2O_3 samples after calcination at 550 °C (* – CeO_2, ○ – SnO_2)

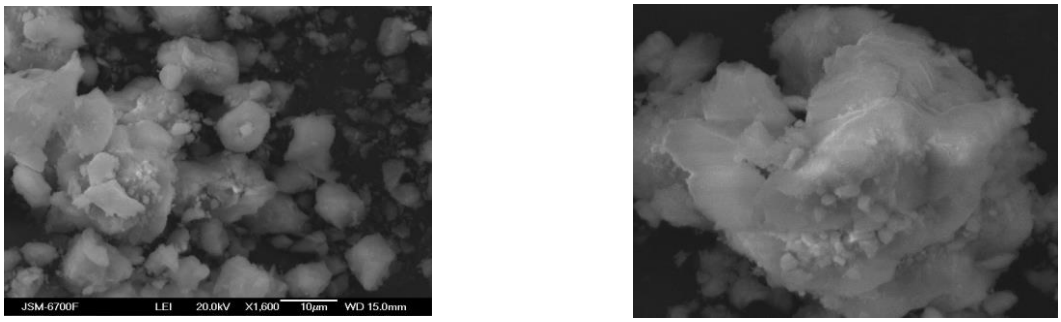

Fig. 3. SEM microphotographs of CeO_2-SnO_2/Al_2O_3 sample

Fig. 4 illustrates the band gap for the synthesized MeO-SnO_2/Al_2O_3 samples obtained from the electronic diffuse reflection spectra. For the SnO_2/Al_2O_3 sample the band gap is 4.5 eV, which indicates the nanosize of tin dioxide particles on the γ-Al_2O_3 surface [14]. Doping with metal oxides shifts the band gap to low energies. Thus, for the MoO_3-SnO_2/Al_2O_3 sample E_g = 3.7 eV, which indicates the presence of amorphous molybdenum oxide on its surface. Since, according to literature data [15], for massive MoO_3, which is in an amorphous state, E_g is in the region of 2.7÷3.2 eV, and the band gap of crystalline orthorhombic MoO_3 is about 1.95 eV. For the CuO-SnO_2/Al_2O_3 sample, E_g = 3.7 eV, which indicates the presence of massive SnO_2 phase on its surface [16]. The band gap for CeO_2 is known to be 2.9 eV [17], which is close to the band gap value of the CeO_2-SnO_2/Al_2O_3 sample (E_g = 3.25 eV). Thus, the UV spectroscopy data are consistent with the X-ray phase analysis data for all synthesized samples.

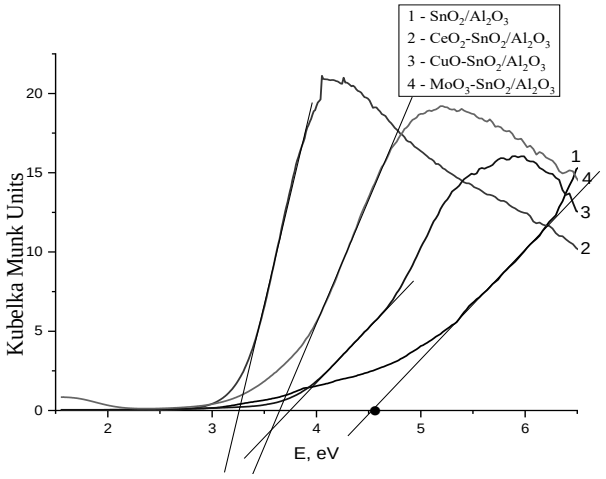

Fig. 4. Optical energy band gap of MeO-SnO_2/Al_2O_3 samples

Table 1. Textural and acidic characteristics of synthesized mixed oxides

Sample	Composition	Textural characteristics			Acidic characteristics	
		Specific surface area, m^2/g	Pore volume, cm^3/g	Average pore radius, nm	Acid strength H_0	Total acidity, mmol/g
SnO_2	-	39	0.07	3.6	+1.5	0.4
Al_2O_3	-	290	0.86	5.3	+3.3	1.2
SnO_2/Al_2O_3	10 % SnO_2	250	0.67	5.7	+1.5	1.3
MoO_3-SnO_2/Al_2O_3	10 % SnO_2, 5 %MoO_3	230	0.63	5.6	+3.3	1.3
CuO-SnO_2/Al_2O_3	10 % SnO_2, 5 %CuO	170	0.55	6.4	-	1.0
CeO_2-SnO_2/Al_2O_3	10 % SnO_2, 5 % CeO_2	200	0.61	6.2	-3.0	0.8

In Table 1 textural characteristics summarized are, as well as strength and concentration of acid sites of synthesized mixed oxides. All samples are mesoporous with a developed surface.

According to the titration results, SnO_2/Al_2O_3 is weakly acid mixed oxide with $H_0 \leq +1.5$ (Table 1). The addition of CeO_2 significantly increases the strength of acid sites of CeO_2-SnO_2/Al_2O_3 samples to $H_0 \leq -3.0$. The acid-base properties of ceria are well known, namely the presence of surface O^{2-} ions as base L-sites and Ce^{4+} ions as acid L-sites, as well as hydroxyl groups as Brønsted basic sites [19]. Strength of Lewis acid sites as surface Ce^{4+} cations is barely dependent on the morphology of the ceria nanocrystals. It was found that octahedra have the smallest number and strength of the base sites [18, 19]. The article [19] presents IR and NMR data that indicate moderate Lewis acid strength of cerium cations on the surface of ceria-based catalysts.

The synthesized MeO-SnO_2/Al_2O_3 samples were further tested as catalysts for the reaction of retro-aldol xylose condensation into methyl lactate (ML) in rotated autoclave (Table 2). According to the results of the products analysis, 100 % xylose conversion occurs only for CeO_2-SnO_2/Al_2O_3 catalyst with a methyl lactate selectivity of 21 %. At the same time, a large amount of acetal and hemiacetal of pyruval are formed. In [20] it was noted that these acetals are the main products in the conversion of dihydroxyacetone-ethanol mixture over typical solid acids Amberlyst 15 and ZrO_2-SiO_2.

It should be noted that almost all tin dioxide was leached out from the surface of the CuO-SnO_2/Al_2O_3 catalyst during the reaction and MoO_3-SnO_2/Al_2O_3 oxide does not provide 100 % conversion of xylose (Table 2). Therefore, CeO_2-SnO_2/Al_2O_3 catalyst was chosen for further studies in flow regime.

Results of xylose conversion carried out in a flow reactor at different temperature on CeO_2-SnO_2/Al_2O_3 catalyst in air flow are presented in Table 3.

Table 2. Xylose conversion to methyl lactate over various catalysts[1]

Catalyst	Conversion of xylose, %	Reaction products			
		ML	Acetals	Fur	Others
SnO_2/Al_2O_3	90	28	19	11	32
MoO_3-SnO_2/Al_2O_3	88	19	55	13	3
CuO-SnO_2/Al_2O_3	78	33	45	-	-
CeO_2-SnO_2/Al_2O_3	100	21	79	-	-

[1] Reaction conditions: 1.1 g xylose, 0.68 g catalyst, 10 g 99 % methanol, 160 °C, 3 h; ML – methyl lactate, Fur– furans, Others – unidentified products

Table 3. Xylose conversion to reaction products at different temperatures on CeO_2-SnO_2/Al_2O_3 catalyst[1]

Temperature, °C	The composition of the reaction products, mol%				
	ML	MG	MF	Fur	Others
160	10	3	-	15	72
170	16	5	6	12	61
180	37	14	13	11	25
190	42	24	15	10	9

[1] Reaction conditions: 4 % xylose solution in a 70 % aqueous methanol solution, 3.0 MPa, L = 3.5 mmol $C_5H_{10}O_5/g_{cat}$/h, air flow; ML – methyl lactate, MG– methyl glycolate, MF – methyl formate, Fur– furans, Others – unidentified products

Conversion of xylose is 100 % in the entire studied temperature range because the signals of D-xylopyranose in the range of 98–62 ppm were not observed in the ^{13}C NMR spectra of reaction products (Fig. 5).

As shown in Table 3, with an increase in the reaction temperature, the selectivity of side methyl formate grows while yield of other by-products decreases. A further increase in, the reaction temperature up to 200 °C leads to

intensive formation of gaseous CO_2. The temperature dependences of yield of targeted ML and MG are shown in Fig. 6.

Thus, at 190 °C, 3.0 MPa in air flow, a complete conversion of xylose occurs with the formation of methyl lactate (42 %) and methyl glycolate (24 %) on the developed CeO_2-SnO_2/Al_2O_3 catalyst at a loading of 3.5 mmol $C_5H_{10}O_5/g_{cat}/h$.

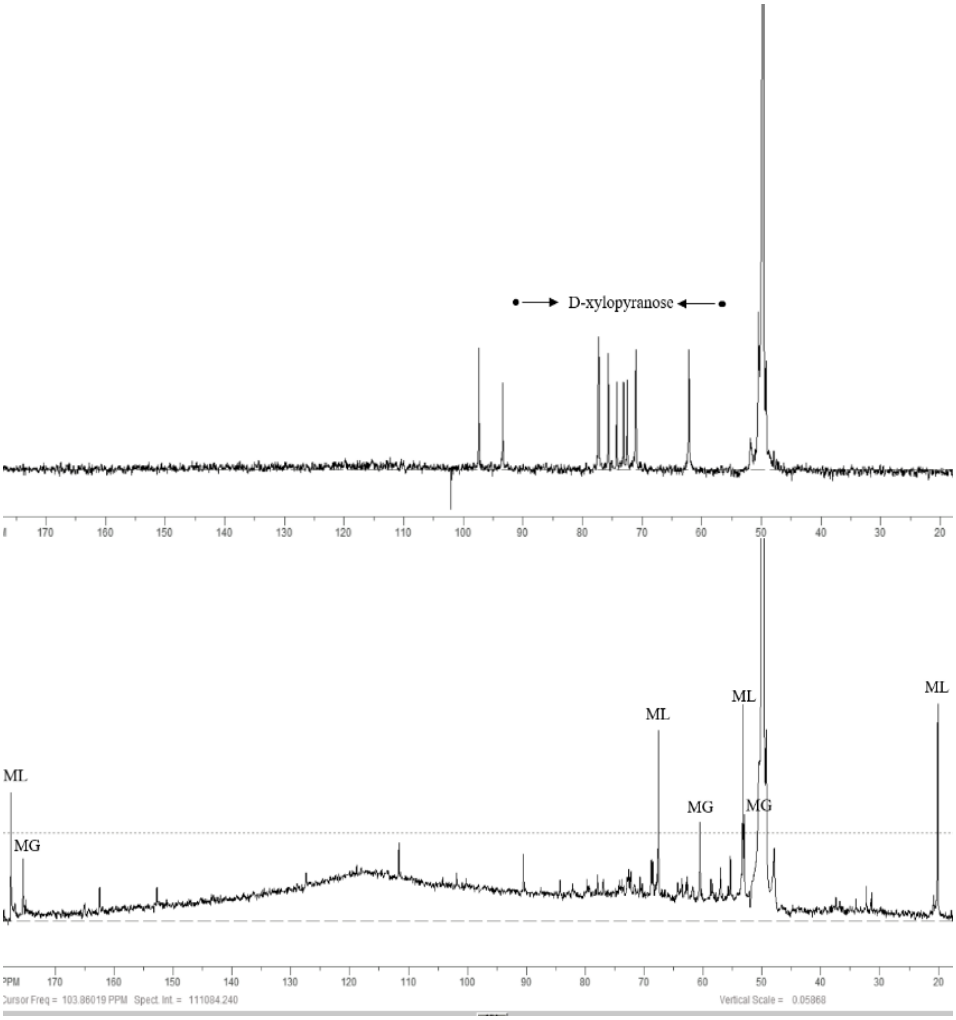

Fig. 5. ^{13}C NMR spectra of xylose (5 % xylose solution in a 70 % aqueous methanol solution) and reaction products

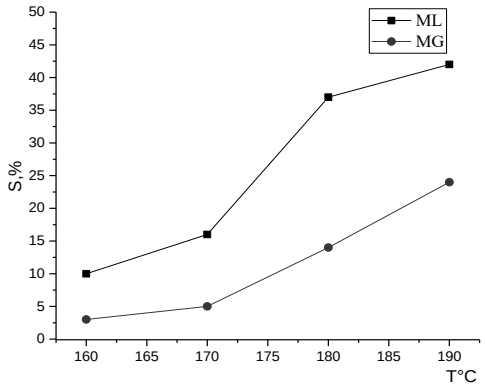

Fig. 6. Methyl lactate and methyl glycolate yields at different temperature on CeO_2-SnO_2/Al_2O_3 catalyst (L = 3.5 mmol $C_5H_{10}O_5/g_{cat}/h$)

The $^{IV}Sn^{4+}$ ions in CeO_2-SnO_2/Al_2O_3 catalyst as Lewis acid sites promote retro-aldol xylose condensation and further Cannizzaro rearrangement of intermediate methyl pyruval hemiacetal into methyl lactate (Scheme 1). And CeO_2 provides selective oxidation of glycol aldehyde formed as a result of aldol decondensation of xylose to methyl glycolate. This involves a two-stage oxidation Mars-Krevelen mechanism, according to which, glycol aldehyde reacts with the original catalyst - an oxidant, and then the catalyst is reoxidized by air oxygen.

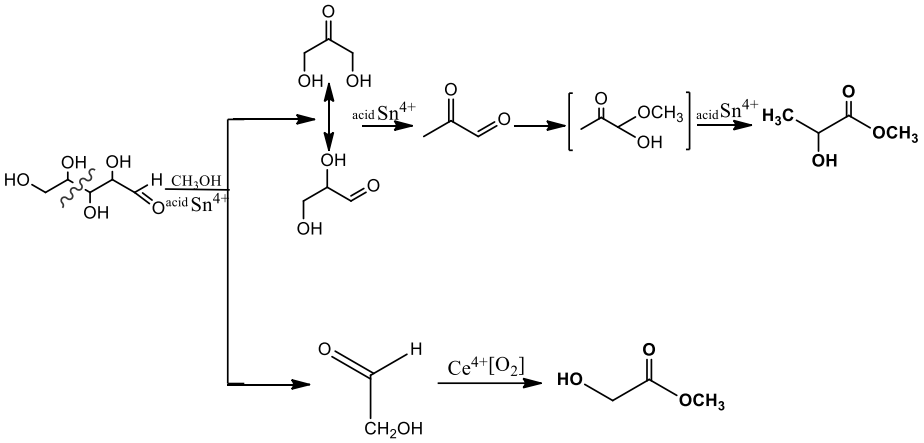

CONCLUSION

Thus, an effective catalyst for the conversion of xylose into methyl esters of glycolic and lactic acids has been proposed. It was shown that as a result of first stage of aldol decondensation of xylose on the acid $^{IV}Sn^{4+}$ L-sites of catalyst, glyceraldehyde and glycol aldehyde are formed. The acid $^{IV}Sn^{4+}$ sites can be obtained by simply impregnating the surface of γ-Al_2O_3 with nanosized tin dioxide particles, which is confirmed by UV spectroscopy data. The same $^{IV}Sn^{4+}$ ions contribute to the last stage of retro-aldol condensation of xylose, namely Cannizzaro rearrangement of intermediate methyl pyruval hemiacetal into methyl lactate. Further doping of SnO_2/Al_2O_3 with oxides having redox properties makes it possible to obtain a catalyst for the oxidation of formed glycol aldehyde to methyl glycolate in methanol solution. It has been found that among the studied oxides namely ceria provides selective oxidation of glycol aldehyde to methyl glycolate. The formation of cubic fluorite phase of CeO_2 with the morphology close to octahedra for CeO_2-SnO_2/Al_2O_3 sample was confirmed by XRD and SEM methods. It was found that 4 wt. % solution of xylose in 70 % methanol is a suitable reaction mixture for obtaining methyl esters of glycolic and lactic acids over proposed CeO_2-SnO_2/Al_2O_3 catalyst at 190 °C/3.0 MPa in air flow. This catalyst provides a complete conversion of xylose with the formation of methyl lactate (42 mol. %) and methyl glycolate (24 mol. %) at load on a catalyst of 3.5 mmol $C_5H_{10}O_5/g_{cat}$/h.

Окиснення суміші ксилоза-метанол в метиллактат та метилгліколат на CeO_2-SnO_2/Al_2O_3 каталізаторі

С.В. Прудіус, Н.Л. Гес, А.Ю. Журавльов, В.В. Брей

Інститут сорбції та проблем ендоекології Національної академії наук України
вул. Генерала Наумова, 13, Київ, 03164, Україна, svitprud@gmail.com

В останні роки розробка каталітичних методів конверсії ксилози як відновлюваної сировини в хімічні речовини з доданою вартістю, такі як естери молочної та гліколевої кислот, є предметом інтенсивних досліджень. Так, метиллактат і метилгліколат використовуються як вихідний матеріал для виробництва лактиду і гліколіду – важливих мономерів для виробництва біорозкладних полімерів. Метою даної роботи був пошук простого ефективного каталізатора для перетворення ксилози в метилові естери молочної та гліколевої кислот. Для цього методом імпрегнування синтезували олововмісний оксид алюмінію, допований оксидами CeO_2, MoO_3 та CuO. Текстурні та структурні параметри одержаних змішаних MeO-SnO_2/Al_2O_3 оксидів оцінено за результатами низькотемпературної адсорбції-десорбції азоту та рентгенофазового аналізу. Формування морфології оксиду церію, близької до октаедра, для зразка CeO_2-SnO_2/Al_2O_3 підтверджено даними рентгенофазового аналізу та мікрофотографіями SEM. Дані УФ-спектроскопії вказують на нанорозмір частинок діоксиду олова на поверхні γ-Al_2O_3. За результатами титрування CeO_2-SnO_2/Al_2O_3 є кислотним змішаним оксидом з $H_0 \leq -3.0$. Каталітичну конверсію розчину ксилози в метанолі проводили в автоклавах, що обертаються, і в проточному реакторі з нержавіючої сталі з нерухомим шаром каталізатора. Продукти цільової реакції $C_5H_{10}O_5+2CH_3OH+1/2O_2=C_4H_8O_3+C_3H_6O_3+2H_2O$ аналізували методом ^{13}C ЯМР. Встановлено, що повна конверсія 4 % розчину ксилози в 70 % водному розчині метанолу відбувається з утворенням метиллактату (42 %) і метилгліколяту (24 %) на розробленому каталізаторі CeO_2-SnO_2/Al_2O_3 з навантаженням 3.5 ммоль $C_5H_{10}O_5/г_{кат}$/год при 190 °C/3.0 МПа в потоці повітря. Запропоновано шлях реакції, а саме: іони $^{IV}Sn^{4+}$ каталізатора CeO_2-SnO_2/Al_2O_3 як кислотні центри Льюїса сприяють ретро-альдольній конденсації ксилози та подальшому перегрупуванню Канніццаро проміжного напівацеталю піровиноградного альдегіду в метиллактат. А CeO_2 забезпечує селективне окиснення гліколевого альдегіду, що утворюється в результаті альдольної деконденсації ксилози, до метилгліколяту.

***Ключові слова**: конверсія ксилози, метиллактат, метилгліколат, змішані оксиди, CeO_2, SnO_2*

REFERENCES

1. Esteban J., Yustos P., Ladero M. Catalytic processes from biomass-derived hexoses and pentoses: a recent literature overview. *Catalysts.* 2018. **8**(12): 637.
2. Lundberg P. *DECOS and SCG Basis for an Occupational Standard Lactate esters.* (Sweden: National Institute for Working Life,1999).
3. Patent US 6326458 B1. Gruber P.R., Hall E.S., Kolstad J.J., Iwen M.L., Benson R.D., Borchardt R.L. Continuous process for the manufacture of lactide and lactide polymers. 2001.
4. Patent UA 145097. Brei V.V., Shchutskyi I.V., Sharanda M.Ye., Varvarin A.M., Levytska S.I., Mylin A.M., Prudius S.V., Zinchenko O.Yu. The method of obtaining lactide from C3 polyols. 2020.
5. Farah Sh., Anderson D.G., Langer R. Physical and mechanical properties of PLA, and their functions in widespread applications – A comprehensive review. *Adv. Drug Delivery Rev*. 2016. **107**: 367.
6. Yang Sh.-B., Chien I.-L. Rigorous Design and Optimization of Methyl Glycolate Production Process through Reactive Distillation Combined with a Middle Dividing-Wall Column. *Ind. Eng. Chem. Res*. 2019. **58**(13): 5215.
7. Prudius S.V., Hes N.L., Mylin A.M., Brei V.V. Continuous conversion of fructose into methyl lactate over SnO_2-ZnO/Al_2O_3 catalyst. *Journal of Chemistry and Technologies*. 2021. **29**(1): 1.
8. Brei V.V., Levytska S.I., Prudius S.V. To the question of oxidation on the surface of oxides: temperature-programmed oxidation of cyclohexanol. *Kataliz ta Naftohimia*. 2022. **33**: 1.
9. Tanabe K, Misono M, Ono Y. *New Solid Acids and Bases – Their Catalytic Properties*. (Amsterdam: Elsevier,1989).
10. Shembel E., Apostolova R., Nagirny V., Kirsanova I., Grebenkin Ph., Lytvyn P. Electrolytic molybdenum oxides in lithium batteries. *J. Solid State Electrochem*. 2005. **9**: 96.

11. Jayalakshmi M., Venugopal N., Phani Raja K., Mohan Rao M. Nano SnO_2–Al_2O_3 mixed oxide and SnO_2-Al_2O_3-carbon composite oxides as new and novel electrodes for super capacitor applications. *J. Power Sources.* 2006. **158**(2): 1538.
12. Gobara H.M., Mohamed R.S., Aboutaleb W.A. A facile synthesis of 3D pyramidal hierarchical CeO_2–Al_2O_3 nanocomposites supported nickel catalyst for cyclohexane dehydrogenation. *Microporous Mesoporous Mater.* 2012. **323**: 111151.
13. Baudin M., Wójcik M., Hermansson K. Dynamics, structure and energetics of the (111), (011) and (001) surfaces of ceria. *Surf. Sci.* 2000. **468**: 51.
14. Prudius S.V., Hes N.L., Brei V.V. Conversion of D-fructose into ethyl lactate over a supported SnO_2–ZnO/Al_2O_3 catalyst. *Colloids Interfaces.* 2019. **3**(16): 16.
15. Bhatia S., Khanna A., Jain R.K., Hirdesh H. Structure-property correlations in molybdenum trioxide thin films and nanoparticles. *Mater. Res. Express*. 2019. **6**: 086409.
16. Razeghizadeh A.R., Zalaghi L., Kazeminezhad I., Rafee V. Growth and Optical Properties Investigation of Pure and Al-doped SnO_2 Nanostructures by Sol-Gel Method. *Iran. J. Chem. Chem. Eng.* 2017. **36**: 1.
17. Ansari S.A., Khan M.M., Ansari M.O., Kalathil S., Lee J., Cho M.H. Band gap engineering of CeO_2 nanostructure using an electrochemically active biofilm for visible light applications. *RSC Adv*. 2014. **4**(32): 16782.
18. Wu Z., Mann A.K.P., Li M., Overbury S.H. Spectroscopic Investigation of Surface-Dependent Acid–Base Property of Ceria Nanoshapes. *J. Phys. Chem. C.* 2015. **119**(13): 7340.
19. Wang X., Li M., Wu Z. In situ spectroscopic insights into the redox and acid-base properties of ceria catalysts. *Chin. J. Catal*. 2021. **42**(12): 2122.

Received 31.01.2024, accepted 03.09.2024